

## Copyright Notice

This paper was published in *Optics Express* and is made available as an electronic reprint with the permission of OSA. The paper can be found at the following URL on the OSA website:  
<http://dx.doi.org/10.1364/OE.19.016890>. Systematic or multiple reproduction or distribution to multiple locations via electronic or other means is prohibited and is subject to penalties under law.

*(Article begins on next page)*

# Direct measurement of the spectral reflectance of OP-SDL gain elements under optical pumping

Carl Borgentun,\* Jörgen Bengtsson, and Anders Larsson

Photonics Laboratory, Department of Microtechnology and Nanoscience (MC2),  
Chalmers University of Technology, Kemivägen 9, 41296 Göteborg, Sweden

[\\*carl.borgentun@chalmers.se](mailto:carl.borgentun@chalmers.se)

**Abstract:** We report on a direct measurement method for acquiring highly precise reflectance spectra of gain elements for semiconductor disk lasers under optical pumping. The gain element acts as an active mirror, and the active mirror reflectance (AMR) was measured with a weak and tunable probe beam coincident on the gain element with a high-power pump beam. In particular, we measured the spectral AMR of a gain element designed to have a broad and flat AMR spectrum by being anti-resonant at the center wavelength and employing a parametrically optimized anti-reflection structure. We were able to confirm that this sophisticated gain element performs according to design, with an almost constant AMR of  $\sim 103\%$  over a wavelength range of nearly 35 nm, very well matching the simulated behavior. Such gain characteristics are useful for optically pumped semiconductor disk lasers (OP-SDLs) designed for broadband tuning and short-pulse generation through mode-locking. The measurement technique was also applied to a conventional resonant periodic gain element designed for fixed wavelength OP-SDL operation; its AMR spectrum is markedly different with a narrow peak, again in good agreement with the simulations.

© 2011 Optical Society of America

**OCIS codes:** (120.5700) Reflection; (140.5960) Semiconductor lasers; (120.3940) Metrology.

---

## References and links

1. B. Rudin, A. Rutz, M. Hoffmann, D. J. H. C. Maas, A.-R. Bellancourt, E. Gini, T. Südmeyer, and U. Keller, "Highly efficient optically pumped vertical-emitting semiconductor laser with more than 20 W average output power in a fundamental transverse mode," *Opt. Lett.* **33**, 2719–2721 (2008).
  2. T.-L. Wang, Y. Kaneda, J. M. Yarborough, J. Hader, J. V. Moloney, A. Chernikov, S. Chatterjee, S. W. Koch, B. Kunert, and W. Stolz, "High-power optically pumped semiconductor laser at 1040 nm," *IEEE Photon. Technol. Lett.* **22**, 661–663 (2010).
  3. A. Wojcik-Jedlinska, K. Pierscinski, A. Jasik, J. Muszalski, and M. Bugajski, "Optical characterisation of vertical-external-cavity surface-emitting lasers (VECSELs)," *Opt. Appl.* **37**, 449–457 (2007).
  4. C. Borgentun, J. Bengtsson, A. Larsson, F. Demaria, A. Hein, and P. Unger, "Optimization of a broadband gain element for a widely tunable high-power semiconductor disk laser," *IEEE Photon. Technol. Lett.* **22**, 978–980 (2010).
  5. J. Paajaste, S. Suomalainen, R. Koskinen, A. Härkönen, M. Guina, and M. Pessa, "High-power and broadly tunable GaSb-based optically pumped VECSELs emitting near 2  $\mu\text{m}$ ," *J. Cryst. Growth* **311**, 1917–1919 (2009).
  6. A.-R. Bellancourt, Y. Barbarin, D. J. H. C. Maas, M. Shafiei, M. Hoffmann, M. Golling, T. Südmeyer, and U. Keller, "Low saturation fluence antiresonant quantum dot SESAMs for MIXSEL integration," *Opt. Express* **17**, 9704–9711 (2009).
  7. L. Coldren and S. Corzine, *Diode Lasers and Photonic Integrated Circuits* (Wiley, 1995).
-

## 1. Introduction

The optically pumped semiconductor disk laser (OP-SDL), or vertical-external-cavity surface-emitting laser (VECSEL), is a laser capable of generating a high-power beam of almost diffraction-limited quality [1,2]. The properties of the spatial modes of the OP-SDL emission are controlled by the external cavity but the power, tuning, and pulse generation characteristics are to a large extent governed by the properties of the semiconductor gain element (GE). It is therefore of utmost importance to be able to measure relevant properties of the GE under the same optical pumping conditions assumed in the design. A common way to experimentally test the design is to perform a spectral reflectance measurement in the absence of optical pumping, i.e. to simply measure the reflectance of a tunable probe beam incident on the "non-active" GE [3]. This is a straight-forward measurement method but reveals little information on the actual performance of the GE under pump excitation. Other methods are based on measurements on the entire OP-SDL, thus including also the external cavity, such as the pump threshold intensity measurements of a tunable OP-SDL in [4], and thus only provide indirect information on the spectral properties of the GE since cavity and saturation effects influence the measurements.

In this paper, we instead directly measure the reflectance of an optically pumped GE, which we refer to as the active mirror reflectance (AMR). This method avoids adverse influences from external cavity effects and enables a direct comparison with design simulations. This comparison is very valuable for assessing different GE designs, particularly those for more advanced functions, such as designs for wide tuning [4,5] or short-pulse generation [6]. Under optical pumping, the AMR is typically just above 100%, with small variations from this value having a large impact on the performance of the OP-SDL. Therefore, the required precision in this measurement is higher than for most reflectance measurements. Also, the need to simultaneously control the size and position of both pump and probe beams complicates the setup, as does the need to provide sufficient cooling of the GE.

## 2. Setup for Measuring the AMR

In the setup, illustrated in Fig. 1, a tunable Ti-sapphire laser is used as a reflectance probe. The output power as a function of the emission wavelength is shown in Fig. 2. The probe beam is attenuated to a maximum power of  $\sim 5$  mW with an absorbing neutral density filter, which also functions as a beam-splitter directing a weak residual reflection onto the collecting lens of a

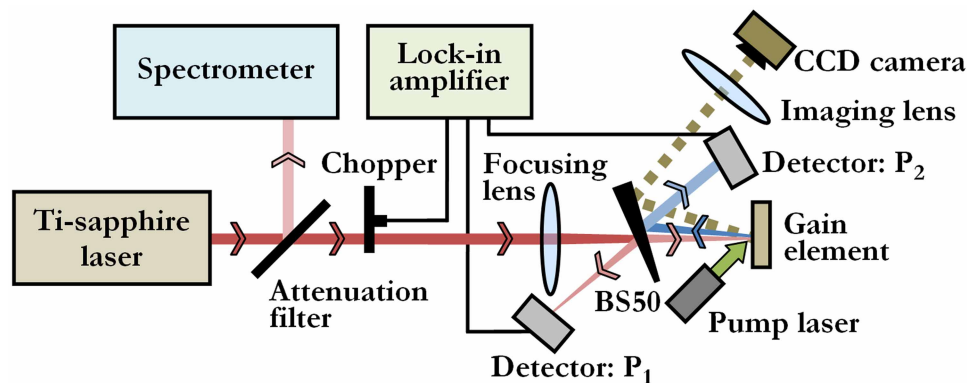


Fig. 1. (Color online) Schematic overview of the measurement setup (BS50: Wedged 50-50 beam-splitter). When aligning the spots from the probe and pump lasers, the top detector is removed in order to image the GE surface with a lens and a CCD camera.

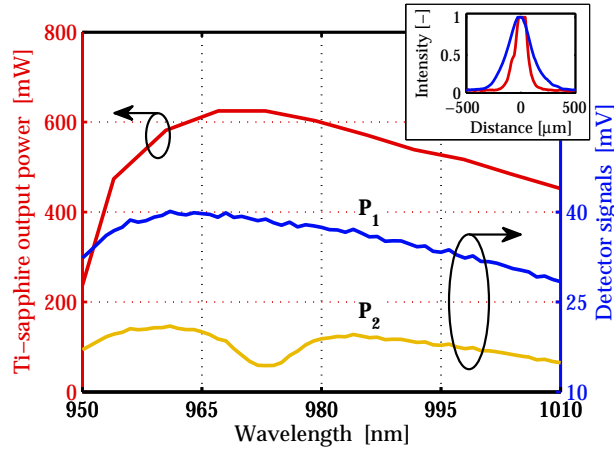


Fig. 2. (Color online) The output power dependence on emission wavelength for the tunable probe laser. Also shown are the signals from the two power detectors for a typical AMR measurement of an unpumped broadband GE. The inset shows the beam intensity cross-sections at the GE from the pump (blue and wider) and probe (red) laser.

fiber spectrometer in order to monitor the emission wavelength. The probe beam is chopped and directed through a focusing lens onto a wedged 50-50 beam-splitter, where a part is reflected onto a power detector. The measured power is denoted by  $P_1$  and is directly proportional to the power incident on the GE at a given wavelength. The part of the probe beam that is transmitted through the beam-splitter is focused onto the GE and reflected back. At the beam-splitter it is reflected again and directed onto a second power detector, where the measured power is denoted by  $P_2$ . Both power detectors are connected to a lock-in amplifier to reduce noise. An example of recorded detector signals is shown in Fig. 2.

The GE is optically pumped by a fiber-coupled 808 nm pump laser that is focused onto the GE with a collimating and focusing lens. In the AMR measurements it is crucial to have good overlap between the focused spots of light from the probe and pump lasers. Thus, before the measurement, the spots of the probe and pump lasers are aligned. During this procedure, the second power detector is removed and a camera objective is used to image the surface of the GE onto a CCD camera. The magnification of the imaging system is calibrated either by measuring a certain distance on the GE as well as in the camera image, or by translating the GE a known distance and measuring the translated distance in the camera image. The objective lens is positioned such that it avoids capturing the specularly reflected probe beam, which otherwise will saturate the detector array of the CCD camera. The size and position of the probe and pump spots are thus monitored by observing the light that is scattered from surface imperfections of the GE, which is of sufficient intensity for convenient detection.

In the actual AMR measurements, some precautions are also taken. The power detectors are slightly tilted so that they do not cause reflections onto each other. Further, any protective glass in front of the detectors is removed to avoid interference effects.

For calibrated measurements, a broadband dielectric mirror with a known reflectance spectrum,  $R_{cal}(\lambda)$ , is used as a reference. At a given wavelength, the measured power  $P_2(\lambda)$  is proportional to both the reflectance of the sample,  $R_{sample}(\lambda)$ , and the optical power incident on the sample, the latter being proportional to the measured power  $P_1(\lambda)$ . We thus have:

$$P_2(\lambda) = \kappa(\lambda) \cdot R_{sample}(\lambda) \cdot P_1(\lambda), \quad (1)$$

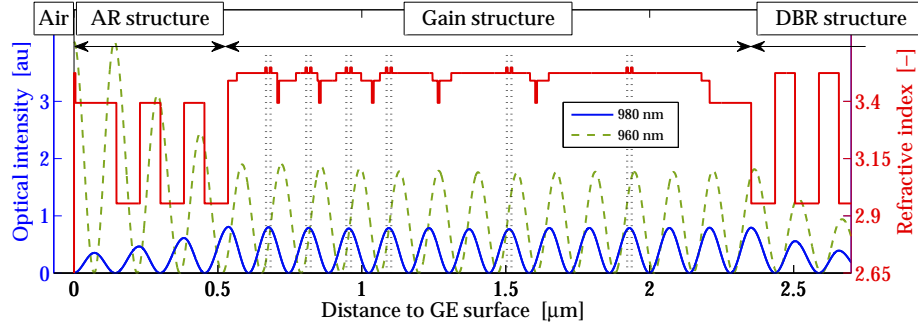


Fig. 3. (Color online) Layer structure of the broadband GE. The QW positions are marked with vertical dotted lines. Also shown is the standing wave of the optical field at two wavelengths: the center wavelength (980 nm) and one of the resonant wavelengths (960 nm).

where we allow for the proportionality constant,  $\kappa(\lambda)$ , to be wavelength dependent since the optical components in the setup are slightly dispersive. The sample reflectance,  $R_{sample}(\lambda)$ , is either the calibration mirror reflectance,  $R_{cal}(\lambda)$ , or the reflectance of the GE,  $AMR(\lambda)$ . Using Eq. 1 for these two cases we can solve for the unknown reflectance of the GE:

$$AMR(\lambda) = \frac{1}{\kappa(\lambda)} \cdot \frac{P_2(\lambda)}{P_1(\lambda)} = R_{cal}(\lambda) \frac{P_1^{cal}(\lambda)}{P_2^{cal}(\lambda)} \cdot \frac{P_2(\lambda)}{P_1(\lambda)}, \quad (2)$$

where the superscript *cal* denotes the measured powers with the calibration mirror inserted.

### 3. Design of the Broadband Gain Element

The design of the broadband GE used in the measurements is described in [4]. In this section we briefly review the design, to illustrate significant differences and additional features compared to a standard GE for a fixed-wavelength continuous wave OP-SDL.

The design aims at broadening the wavelength coverage of a tunable OP-SDL by engineering the GE for broad and flat gain of sufficient magnitude under appropriate pumping conditions. This is in contrast to a GE for a conventional fixed-wavelength OP-SDL which provides gain over a narrow band of wavelengths.

A numerical model capable of calculating the AMR spectrum of the GE at given pump wavelength and intensity was developed. The model is based on the transfer matrix method and accounts for optical gain/absorption in the quantum wells (QWs) through the imaginary part of the refractive index. Gain/absorption calculations included the effects of valence band splitting through strain and quantum size effects, bandgap renormalization, and exciton effects [7]. The numerical model was used to optimize the layer structure of the (InGa)As/(AlGa)As-based GE to provide enough AMR to compensate for the assumed optical cavity losses over a wide ( $\sim 40$  nm) range of wavelengths. This was achieved primarily by designing the GE subcavity, formed by the air/semiconductor interface and the distributed Bragg reflector (DBR), to be antiresonant at the center wavelength of 980 nm while resonance wavelengths were positioned on either side of the center wavelength, at approximately 960 and 1000 nm. The QWs have their gain peak at the center wavelength and the standing wave maxima of the optical field are aligned with the QWs at this wavelength. As the wavelength is tuned from the center wavelength, the reduction of QW gain and the misalignment of the optical field with the QWs are compensated for by the increasing amplitude of the optical field in the subcavity as it becomes increasingly

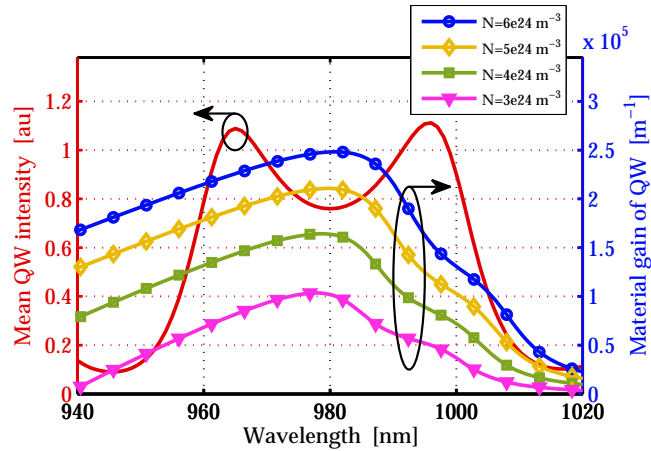


Fig. 4. (Color online) Variation of the average optical intensity in the QWs with wavelength for the broadband GE. The curves with markers are calculated material gain spectra of a single QW for a selection of carrier densities.

resonant. This broadens the effective gain bandwidth of the GE. Finally, a parametrically optimized anti-reflection (AR) structure was included to fine-tune the design and approach the target AMR spectrum.

The design of the optimized broadband GE is shown in Fig. 3, together with the standing wave of the optical field at two wavelengths: the antiresonant center wavelength (980 nm) and one of the resonant wavelengths (960 nm). Fig. 4 shows how the larger intensity of the optical field at resonance increases the optical intensity in the QWs although the peaks of the standing wave are misaligned with the QWs. Fig. 4 also shows how the higher gain in the QWs compensates for the lower optical field intensity at the center wavelength to create a broad AMR spectrum with a value exceeding 100% over the desired wavelength range. Finally, the AR structure flattens the AMR spectrum to very nearly the target (103% over 40 nm), as shown in Fig. 5. Also shown in this figure is the AMR spectrum for a conventional GE, without the AR structure and being resonant at the fixed operating wavelength of 980 nm.

Considering the complexity of the design, the uncertainties in numerical values of materials parameters and the limited accuracy of the epitaxial growth, an experimental confirmation of the expected performance is highly valuable. This was done using the measurement technique presented in the preceding section. The results are presented in the following section.

#### 4. Measurements and Results

Measurements were performed on the broadband GE as well as on a conventional GE designed according to standard design principles, i.e. with the GE resonant for the center wavelength and without an AR structure. Since the probe beam should be focused to a spot smaller than the spot of the pump laser beam, so that the pump intensity is roughly equal over the entire cross section of the probe beam, while the pump intensity must be high enough to populate the QWs to the desired degree, the size of the probe spot is limited by the available pump power. In our case, the probe beam was focused to a  $\sim 220 \mu\text{m}$  diameter spot on the GE using a standard plano-convex lens with 100 mm focal length, while the pump beam was focused to a  $\sim 450 \mu\text{m}$  diameter spot. The GE was mounted on a Peltier-cooled copper heat-sink with liquid cooling and the temperature of the mount was set to  $-5^\circ\text{C}$ . The calibration mirror was a commercial

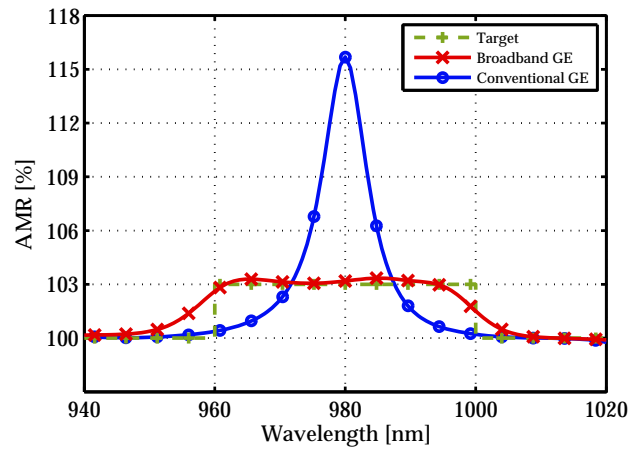


Fig. 5. (Color online) Simulated AMR spectra: the target AMR spectrum (a flat-top spectrum with an AMR of 103% over a wavelength interval of 40 nm), the AMR spectrum for the broadband GE, and for comparison, the AMR spectrum for a standard GE for a fixed-wavelength OP-SDL at the same pump intensity.

dielectric broadband mirror with a specified reflectance slowly varying between 99.6% and 99.7% within the entire wavelength interval.

Results from measurements on the conventional GE, shown in Fig. 6, show a narrow but strong AMR peak close to the center wavelength of 980 nm. The peak redshifts slightly with increasing pump intensity due to an increasing temperature of the GE. The simulations, also shown in Fig. 6, are in very good agreement with the measurements. For best fit, the ratio between the pump intensities in the simulations is somewhat smaller than between the pump powers in the measurements. This can be attributed to a slight increase of the size of the focused spot of the pump beam and an increasing temperature of the GE with increasing pump power, which was not accounted for in the simulations. The large absorption dip visible at  $\sim 965$  nm for zero pump intensity is due to exciton absorption. However, even at low pump powers the excitons are efficiently screened by the generated carriers and exciton effects are no longer visible in the spectra. The lower absorption at resonance at zero pump power in the measurements is attributed to a slightly larger separation between the subcavity resonance and the QW absorption edge compared to the design. The measurements clearly demonstrate that this GE is suitable for OP-SDLs operating continuously at a fixed wavelength.

In contrast, results from the measurements on the broadband GE, shown in Fig. 7, illustrate the much wider range of wavelengths over which sufficient AMR is achieved under optical pumping. Moreover, at moderate or high pump powers, the AMR spectrum tends to have a flat-top shape. Such characteristics are useful for widely tunable OP-SDLs with reduced variation of the output power with wavelength at constant pump power. For comparison, simulated AMR spectra are also shown in Fig. 7. The agreement between measurements and simulations is striking. The exciton absorption dip at zero pump power is present also in this GE, but since one of the subcavity resonances (at 960 nm) is now very close to the exciton resonance wavelength the absorption dip is much larger.

The accuracy of the measurement is mainly determined by the accuracy of the calibration mirror reflectance,  $R_{cal}(\lambda)$ . Since we use a calibration mirror for all wavelengths, many potential sources of error, such as dispersion in optical components and long-term drift in probe beam output power, are canceled and the measurement is robust and precise. The noise that



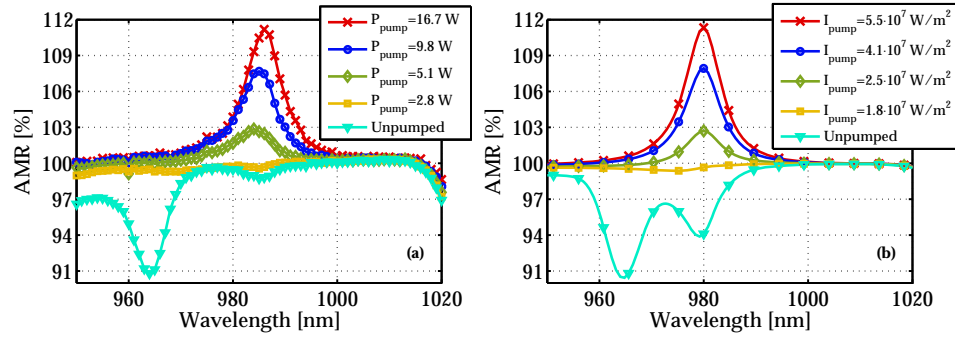


Fig. 6. (Color online) (a) AMR measurements of a conventional GE for different incident pump powers. (b) AMR simulations of the same conventional GE for different incident pump intensities.

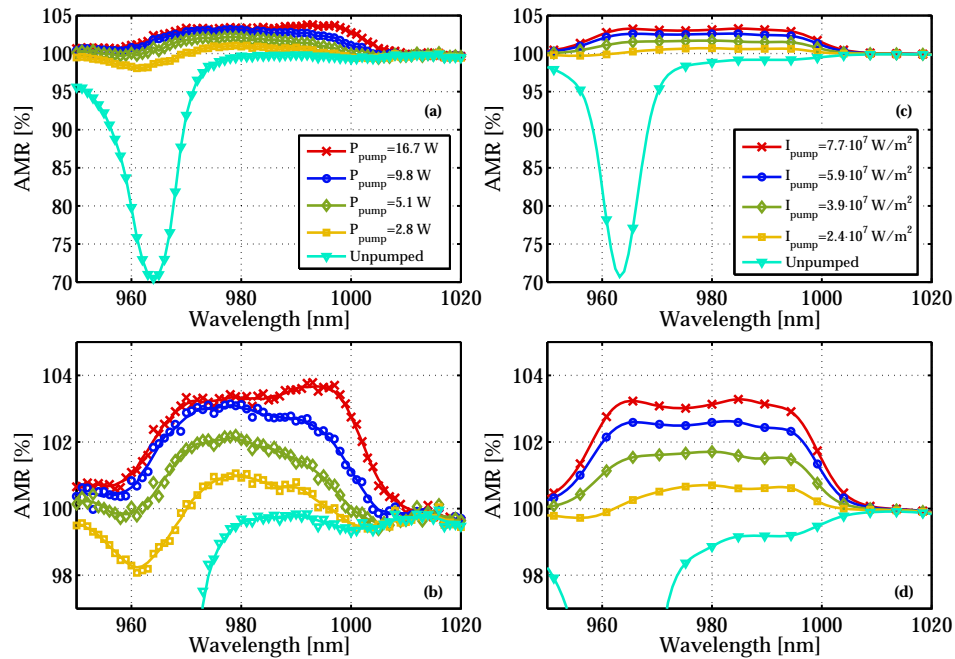


Fig. 7. (Color online) (a) AMR measurements of a broadband GE for different incident pump powers. (b) Zoom-in of above figure. The markers represent data points and the curves are smooth curve fits to the data points. (c) AMR simulations of the same broadband GE for different incident pump intensities. (d) Zoom-in of above figure.



nonetheless can be seen in the zoom-in of the measured AMR is mostly due to temporal fluctuations in the output power of the Ti-sapphire laser between the measurements of  $P_1$  and  $P_2$ , which were sequentially measured with a separation of  $\sim 0.6$  seconds. As a measure of this noise, the root-mean-square of the difference between the data points and the smoothed curve fits in Fig. 7 is  $\sim 0.13$  percentage points.

## 5. Conclusions

We have presented a method for measuring the spectral reflectance characteristics of an OP-SDL gain element under pump excitation. The method is accurate enough to produce absolute reflectance values which allow for a direct comparison with simulated reflectance spectra. With this measurement technique we have been able to confirm that a gain element designed for broadband gain and tuning performs according to design, i.e. having a broad and flat reflectance exceeding that needed to overcome the cavity loss over a wide range of wavelengths under appropriate pumping conditions.

## Acknowledgement

The authors would like to thank Hans Lindberg of Osram Opto Semiconductors for initial discussions.